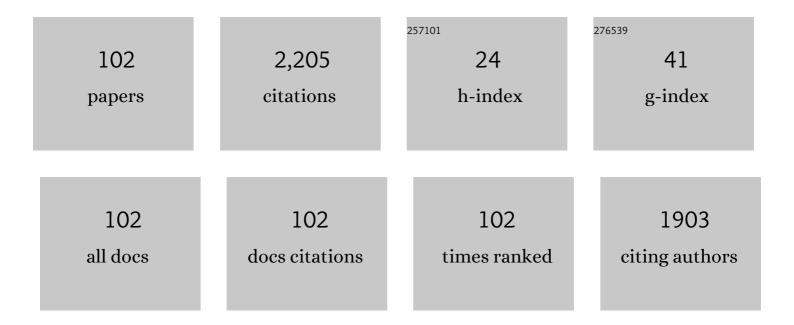
Sabee Molloi

List of Publications by Year in descending order

Source: https://exaly.com/author-pdf/8068114/publications.pdf Version: 2024-02-01



SAREE MOLLOL

#	Article	IF	CITATIONS
1	Absolute cerebral blood flow: Assessment with a novel low-radiation-dose dynamic CT perfusion technique in a swine model. Journal of Neuroradiology, 2022, 49, 173-179.	0.6	2
2	Breast Arterial Calcification: a Novel Cardiovascular Risk Enhancer Among Postmenopausal Women. Circulation: Cardiovascular Imaging, 2022, 15, e013526.	1.3	23
3	Contrast timing optimization of a two-volume dynamic CT pulmonary perfusion technique. Scientific Reports, 2022, 12, 8212.	1.6	1
4	Breast Arterial Calcification Is Not Associated with Mild Cognitive Impairment or Incident All-Cause Dementia Among Postmenopausal Women: The MINERVA Study. Journal of Women's Health, 2021, 30, 848-856.	1.5	1
5	Quantification of water and lipid density with dual-energy mammography: validation in postmortem breasts. European Radiology, 2021, 31, 938-946.	2.3	0
6	Characterization of arterial plaque composition with dual energy computed tomography: a simulation study. International Journal of Cardiovascular Imaging, 2021, 37, 331-341.	0.7	6
7	Combining perfusion and angiography with a low-dose cardiac CT technique: a preliminary investigation in a swine model. International Journal of Cardiovascular Imaging, 2021, 37, 1767-1779.	0.7	3
8	No Association Between Bone Mineral Density and Breast Arterial Calcification Among Postmenopausal Women. Journal of the Endocrine Society, 2020, 4, bvz026.	0.1	3
9	Vessel-specific coronary perfusion territories using a CT angiogram with a minimum cost path technique and its direct comparison to the American Heart Association 17-segment model. European Radiology, 2020, 30, 3334-3345.	2.3	4
10	Dynamic pulmonary CT perfusion using first-pass analysis technique with only two volume scans: Validation in a swine model. PLoS ONE, 2020, 15, e0228110.	1,1	10
11	Timing optimization of low-dose first-pass analysis dynamic CT myocardial perfusion measurement: validation in a swine model. European Radiology Experimental, 2019, 3, 16.	1.7	14
12	Kidney function, proteinuria and breast arterial calcification in women without clinical cardiovascular disease: The MINERVA study. PLoS ONE, 2019, 14, e0210973.	1.1	7
13	Low-Radiation-Dose Stress Myocardial Perfusion Measurement Using First-Pass Analysis Dynamic Computed Tomography. Investigative Radiology, 2019, 54, 774-780.	3.5	8
14	Contrast-to-Noise Ratio Optimization in Coronary Computed Tomography Angiography: Validation in a Swine Model. Academic Radiology, 2019, 26, e115-e125.	1.3	10
15	A phantom based evaluation of vessel lumen area quantification for coronary CT angiography. International Journal of Cardiovascular Imaging, 2019, 35, 551-557.	0.7	3
16	Initial evaluation of three-dimensionally printed patient-specific coronary phantoms for CT-FFR software validation. Journal of Medical Imaging, 2019, 6, 1.	0.8	8
17	MON-515 Lack Of Association Between Bone Mineral Density And Breast Arterial Calcification: The Minerva Study. Journal of the Endocrine Society, 2019, 3, .	0.1	0
18	MultlethNic Study of BrEast ARterial Calcium Gradation and CardioVAscular Disease: cohort recruitment and baseline characteristics. Annals of Epidemiology, 2018, 28, 41-47.e12.	0.9	24

#	Article	IF	CITATIONS
19	Comprehensive Assessment of Coronary Artery Disease by Using First-Pass Analysis Dynamic CT Perfusion: Validation in a Swine Model. Radiology, 2018, 286, 93-102.	3.6	23
20	Quantification of vessel-specific coronary perfusion territories using minimum-cost path assignment and computed tomography angiography: Validation in a swine model. Journal of Cardiovascular Computed Tomography, 2018, 12, 425-435.	0.7	15
21	Association of Breast Arterial Calcification Presence and Gradation with the Ankle-Brachial Index among Postmenopausal Women. The European Journal of Cardiovascular Medicine, 2018, 5, 544-551.	1.0	2
22	Detecting Cardiovascular Disease from Mammograms With Deep Learning. IEEE Transactions on Medical Imaging, 2017, 36, 1172-1181.	5.4	159
23	Breast-density measurement using photon-counting spectral mammography. Medical Physics, 2017, 44, 3579-3593.	1.6	16
24	Quantitative contrastâ€enhanced spectral mammography based on photonâ€counting detectors: A feasibility study. Medical Physics, 2017, 44, 3939-3951.	1.6	6
25	Accurate quantification of vessel cross-sectional area using CT angiography: a simulation study. International Journal of Cardiovascular Imaging, 2017, 33, 411-419.	0.7	6
26	Quantification of breast lesion compositions using lowâ€dose spectral mammography: A feasibility study. Medical Physics, 2016, 43, 5527-5536.	1.6	2
27	Functional Assessment of Coronary Artery Disease Using Whole-Heart Dynamic Computed Tomographic Perfusion. Circulation: Cardiovascular Imaging, 2016, 9, .	1.3	23
28	TICMR: Total Image Constrained Material Reconstruction via Nonlocal Total Variation Regularization for Spectral CT. IEEE Transactions on Medical Imaging, 2016, 35, 2578-2586.	5.4	41
29	Microcalcification detectability using a benchâ€ŧop prototype photonâ€counting breast CT based on a Si strip detector. Medical Physics, 2015, 42, 4401-4410.	1.6	7
30	Demonstration of a non-contact x-ray source using an inductively heated pyroelectric accelerator. Nuclear Instruments and Methods in Physics Research, Section A: Accelerators, Spectrometers, Detectors and Associated Equipment, 2015, 779, 124-131.	0.7	4
31	Breast Density Evaluation Using Spectral Mammography, Radiologist Reader Assessment, and Segmentation Techniques. Academic Radiology, 2015, 22, 1052-1059.	1.3	12
32	Determination of culprit coronary artery branches using hemodynamic indices from angiographic images. International Journal of Cardiovascular Imaging, 2015, 31, 11-19.	0.7	1
33	Dynamic CT perfusion measurement in a cardiac phantom. International Journal of Cardiovascular Imaging, 2015, 31, 1451-1459.	0.7	16
34	Quantification of breast density using dual-energy mammography with liquid phantom calibration. Physics in Medicine and Biology, 2014, 59, 3985-4000.	1.6	7
35	Postmortem validation of breast density using dualâ€energy mammography. Medical Physics, 2014, 41, 081917.	1.6	12
36	Characteristic performance evaluation of a photon counting Si strip detector for low dose spectral breast CT imaging. Medical Physics, 2014, 41, 091903.	1.6	23

#	Article	IF	CITATIONS
37	Breast Tissue Characterization with Photon-counting Spectral CT Imaging: A Postmortem Breast Study. Radiology, 2014, 272, 731-738.	3.6	21
38	Breast tissue decomposition with spectral distortion correction: A postmortem study. Medical Physics, 2014, 41, 101901.	1.6	13
39	A high-resolution photon-counting breast CT system with tensor-framelet based iterative image reconstruction for radiation dose reduction. Physics in Medicine and Biology, 2014, 59, 6005-6017.	1.6	18
40	Characterization of energy response for photonâ€counting detectors using xâ€ray fluorescence. Medical Physics, 2014, 41, 121902.	1.6	30
41	Performance of a hybrid pyroelectric LiNbO3 and TiO2 nanotubes X-ray source. Review of Scientific Instruments, 2013, 84, 073301.	0.6	3
42	Breast Arterial Calcification: a New Marker of Cardiovascular Risk?. Current Cardiovascular Risk Reports, 2013, 7, 126-135.	0.8	41
43	An angiographic technique for coronary fractional flow reserve measurement: in vivo validation. International Journal of Cardiovascular Imaging, 2013, 29, 535-544.	0.7	10
44	Measurement of breast tissue composition with dual energy coneâ€beam computed tomography: A postmortem study. Medical Physics, 2013, 40, 061902.	1.6	21
45	Breast density quantification with cone-beam CT: a post-mortem study. Physics in Medicine and Biology, 2013, 58, 8573-8591.	1.6	15
46	Tightâ€frame based iterative image reconstruction for spectral breast CT. Medical Physics, 2013, 40, 031905.	1.6	66
47	Reply to "Letter to the editor: â€~A novel angiographic fractional flow reserve'― American Journal of Physiology - Heart and Circulatory Physiology, 2013, 304, H1176-H1176.	1.5	1
48	Breast density quantification using magnetic resonance imaging (MRI) with bias field correction: A postmortem study. Medical Physics, 2013, 40, 122305.	1.6	11
49	Quantification of absolute coronary flow reserve and relative fractional flow reserve in a swine animal model using angiographic image data. American Journal of Physiology - Heart and Circulatory Physiology, 2012, 303, H401-H410.	1.5	11
50	Breast composition measurement with a cadmium-zinc-telluride based spectral computed tomography system. Medical Physics, 2012, 39, 1289-1297.	1.6	29
51	Imageâ€based spectral distortion correction for photon ounting xâ€ray detectors. Medical Physics, 2012, 39, 1864-1876.	1.6	46
52	Characterization and optimization of pyroelectric X-ray sources using Monte Carlo spectral models. Nuclear Instruments and Methods in Physics Research, Section A: Accelerators, Spectrometers, Detectors and Associated Equipment, 2012, 689, 47-51.	0.7	9
53	Dual-dictionary learning-based iterative image reconstruction for spectral computed tomography application. Physics in Medicine and Biology, 2012, 57, 8217-8229.	1.6	60
54	Quantification of breast density with spectral mammography based on a scanned multi-slit photon-counting detector: a feasibility study. Physics in Medicine and Biology, 2012, 57, 4719-4738.	1.6	51

#	Article	IF	CITATIONS
55	Estimation of coronary artery hyperemic blood flow based on arterial lumen volume using angiographic images. International Journal of Cardiovascular Imaging, 2012, 28, 1-11.	0.7	17
56	Quantification of fractional flow reserve based on angiographic image data. International Journal of Cardiovascular Imaging, 2012, 28, 13-22.	0.7	21
57	Segmentation and quantification of materials with energy discriminating computed tomography: A phantom study. Medical Physics, 2011, 38, 228-237.	1.6	38
58	Least squares parameter estimation methods for material decomposition with energy discriminating detectors. Medical Physics, 2011, 38, 245-255.	1.6	57
59	Elevated oxidative stress and endothelial dysfunction in right coronary artery of right ventricular hypertrophy. Journal of Applied Physiology, 2011, 110, 1674-1681.	1.2	20
60	Dynamic dual-energy chest radiography: a potential tool for lung tissue motion monitoring and kinetic study. Physics in Medicine and Biology, 2011, 56, 1191-1205.	1.6	20
61	Quantification of coronary microvascular resistance using angiographic images for volumetric blood flow measurement: in vivo validation. American Journal of Physiology - Heart and Circulatory Physiology, 2011, 300, H2096-H2104.	1.5	12
62	Assessment of coronary microcirculation in a swine animal model. American Journal of Physiology - Heart and Circulatory Physiology, 2011, 301, H402-H408.	1.5	12
63	Radiation dose reduction using a CdZnTeâ€based computed tomography system: Comparison to flatâ€panel detectors. Medical Physics, 2010, 37, 1225-1236.	1.6	74
64	Quantification of breast density with dual energy mammography: An experimental feasibility study. Medical Physics, 2010, 37, 793-801.	1.6	43
65	Reproducibility of Breast Arterial Calcium Mass Quantification Using Digital Mammography. Academic Radiology, 2009, 16, 275-282.	1.3	22
66	Allometric scaling in the coronary arterial system. International Journal of Cardiovascular Imaging, 2008, 24, 771-781.	0.7	15
67	Estimation of regional myocardial mass at risk based on distal arterial lumen volume and length using 3D micro-CT images. Computerized Medical Imaging and Graphics, 2008, 32, 488-501.	3.5	22
68	Determination of fractional flow reserve (FFR) based on scaling laws: a simulation study. Physics in Medicine and Biology, 2008, 53, 3995-4011.	1.6	13
69	Quantification of breast density with dual energy mammography: A simulation study. Medical Physics, 2008, 35, 5411-5418.	1.6	31
70	Quantification of breast arterial calcification using full field digital mammography. Medical Physics, 2008, 35, 1428-1439.	1.6	27
71	Regional blood flow analysis and its relationship with arterial branch lengths and lumen volume in the coronary arterial tree. Physics in Medicine and Biology, 2007, 52, 1495-1503.	1.6	14
72	Quantitative coronary angiography using image recovery techniques for background estimation in unsubtracted images. Medical Physics, 2007, 34, 4003-4015.	1.6	7

#	Article	IF	CITATIONS
73	Automated Technique for Angiographic Determination of Coronary Blood Flow and Lumen Volume. Academic Radiology, 2006, 13, 186-194.	1.3	6
74	Optimization of a flat-panel based real time dual-energy system for cardiac imaging. Medical Physics, 2006, 33, 1562-1568.	1.6	21
75	Feasibility of real time dual-energy imaging based on a flat panel detector for coronary artery calcium quantification. Medical Physics, 2006, 33, 1612-1622.	1.6	27
76	Photon counting computed tomography: Concept and initial results. Medical Physics, 2005, 32, 427-436.	1.6	88
77	Scanning-slit photon counting x-ray imaging system using a microchannel plate detector. Medical Physics, 2004, 31, 1061-1071.	1.6	20
78	Area beam equalization. Academic Radiology, 2004, 11, 377-389.	1.3	3
79	Regional volumetric coronary blood flow measurement by digital angiography. Academic Radiology, 2004, 11, 757-766.	1.3	23
80	Effect of area x-ray beam equalization on image quality and dose in digital mammography. Physics in Medicine and Biology, 2004, 49, 3539-3557.	1.6	10
81	Evaluation of a photon-counting x-ray imaging detector based on microchannel plates for mammography applications. , 2004, 5368, 726.		1
82	Assessment of vasoreactivity using videodensitometry coronary angiography. International Journal of Cardiovascular Imaging, 2003, 19, 271-279.	0.2	2
83	Automatic 3D vascular tree construction in CT angiography. Computerized Medical Imaging and Graphics, 2003, 27, 469-479.	3.5	64
84	X-ray imaging with "edge-on―microchannel plate detector: first experimental results. Nuclear Instruments and Methods in Physics Research, Section A: Accelerators, Spectrometers, Detectors and Associated Equipment, 2003, 510, 401-405.	0.7	8
85	Effect of vessel orientation on videodensitometry quantitative coronary arteriography. Medical Physics, 2003, 30, 2862-2868.	1.6	1
86	Patient-specific Region-of-Interest Fluoroscopy Device for X-ray Dose Reduction. Radiology, 2003, 226, 585-592.	3.6	6
87	Reshapable physical modulator for intensity modulated radiation therapy. Medical Physics, 2002, 29, 2222-2229.	1.6	20
88	Vascular tree object segmentation by deskeletonization of valley courses. Computerized Medical Imaging and Graphics, 2002, 26, 419-428.	3.5	14
89	Applications of "edge-on―illuminated porous plate detectors for diagnostic X-ray imaging. Nuclear Instruments and Methods in Physics Research, Section A: Accelerators, Spectrometers, Detectors and Associated Equipment, 2002, 487, 676-684.	0.7	2
90	In vivo validation of the design rules of the coronary arteries and their application in the assessment of diffuse disease. Physics in Medicine and Biology, 2002, 47, 977-93.	1.6	35

#	ARTICLE	IF	CITATIONS
91	Quantification of Coronary Artery Lumen Volume by Digital Angiography. Circulation, 2001, 104, 2351-2357.	1.6	33
92	X-ray Beam Equalization: Feasibility and Performance of an Automated Prototype System in a Phantom and Swine. Radiology, 2001, 221, 668-675.	3.6	11
93	Scatter and veiling glare estimation based on sampled primary intensity. Medical Physics, 1999, 26, 2301-2310.	1.6	15
94	Area x-ray beam equalization for digital angiography. Medical Physics, 1999, 26, 2684-2692.	1.6	15
95	On the design of the coronary arterial tree: a generalization of Murray's law. Physics in Medicine and Biology, 1999, 44, 2929-2945.	1.6	170
96	Absolute volumetric coronary blood flow measurement with digital subtraction angiography. International Journal of Cardiovascular Imaging, 1998, 14, 137-145.	0.2	38
97	Measurement of a cross-sectional area of normal and stenotic arteries with videodensitometric quantitative arteriography and intravascular ultrasound. Academic Radiology, 1997, 4, 245-252.	1.3	7
98	Quantification of Volumetric Coronary Blood Flow With Dual-Energy Digital Subtraction Angiography. Circulation, 1996, 93, 1919-1927.	1.6	43
99	In-vivo validation of videodensitometric coronary cross-sectional area measurement using dual-energy digital subtraction angiography. International Journal of Cardiovascular Imaging, 1995, 11, 223-231.	0.2	12
100	Accuracy of Quantifying Coronary Hydroxyapatite with Electron Beam Tomography. Investigative Radiology, 1994, 29, 733-738.	3.5	44
101	Absolute volumetric blood flow measurements using dual-energy digital subtraction angiography. Medical Physics, 1993, 20, 85-91.	1.6	15
102	Quantification of coronary arterial calcium by dual energy digital subtraction fluoroscopy. Medical Physics, 1991, 18, 295-298.	1.6	28